Chaos, Solitons and Fractals 81 (2015) 103–110

Contents lists available at ScienceDirect

Chaos, Solitons and Fractals

Nonlinear Science, and Nonequilibrium and Complex Phenomena

journal homepage: www.elsevier.com/locate/chaos

A robust method to estimate the *b*-value of the magnitude–frequency distribution of earthquakes

Qinghua Han [a,b], Lichen Wang [a,b], Jie Xu [a,b,*], Alberto Carpinteri [c], Giuseppe Lacidogna [c]

[a] School of Civil Engineering, Tianjin University, Tianjin 300072, China
[b] Key Laboratory of Coast Civil Structure Safety (Tianjin University), Ministry of Education, Tianjin 300072, China
[c] Department of Structural, Geotechnical and Building Construction, Politecnico di Torino, Italy

ARTICLE INFO

Article history:
Received 29 September 2013
Accepted 7 September 2015
Available online 27 September 2015

Keywords:
Magnitude–frequency distribution
b-Value
Least square regression
Maximum likelihood estimation
Robust fitting method
Earthquake precusor

ABSTRACT

The methods to estimate the *b*-value of the magnitude–frequency distribution are analyzed based on a certain period of earthquakes in the central region of China. According to the problems in the traditional methods, least square regression method and maximum likelihood estimation mathod, a robust fitting method to estimate the *b*-value is proposed. The least square regression method is suggested not to be used in the future for its unstability and great deviation from the linerity to the extrem events. The use of maximum likelihood estimation method needs a high accurate assessment of the magnitude of completeness. Compared with the two traditional methods, the proposed method can not only provide a stable and reliable *b*-value, but also has a good sensitivity to the occurrence of earthquakes with large magnitudes. The variation of *b*-value as an earthquake precursor is applied successfully in our study, and the proposed robust fitting method is shown to be more efficient than the maximum likelihood estimation method.

1. Introduction

In spite of existence of breaks in earthquakes scaling caused by temporal and spatial heterogeneity [1], the assumption of self-similarity of the earthquakes process is found in most cases. Self-similarity is consistent with the observed linear *b*-value relation of the Gutenberg (GR) law [2],

$$\log_{10} N(M) = a - bM, \tag{1}$$

where $N(M)$ is the number of events with magnitude equal to or greater than M, and a and b are real constants that may vary in space and time. It should be note that often instead of magnitude M the log of seismic moment or log of seismic energy is used. Parameter a is a measure of seismic activity that depends on the size of the area, the length of the observation period, the largest seismic magnitude, and *b*-value is a constant parameter that determines the rate of fall in the frequency of events with increasing magnitude. A higher *b* value means that a smaller fraction of the total earthquakes occurs at the higher magnitudes, whereas a lower *b* value implies a larger fraction.

The scientific importance of the Gutenberg (GR) law is ubiquitous. It emerges in a variety of tectonic settings and depth ranges, in seismic catalogs ranging from a few months to centuries, in natural as well as induced seismicity and in seismic hazard studies. The significance of the *b* parameter for quantifying seismicity [3] or for dealing with problems of earthquake prediction [4] has been recognized widely by seismologists. Significant spatial and temporal variations of *b*-value are usually attributed to many processes, such as the fault heterogeneity [5], the stress level imposed on rocks [6],

* Corresponding author at: School of Civil Engineering, Tianjin University, China/Key Laboratory of Coast Civil Structure Safety (Tianjin University), Ministry of Education, Tianjin 300072, China. Tel.: +86 2227402192.
E-mail address: jxu@tju.edu.cn (J. Xu).

http://dx.doi.org/10.1016/j.chaos.2015.09.004
0960-0779/

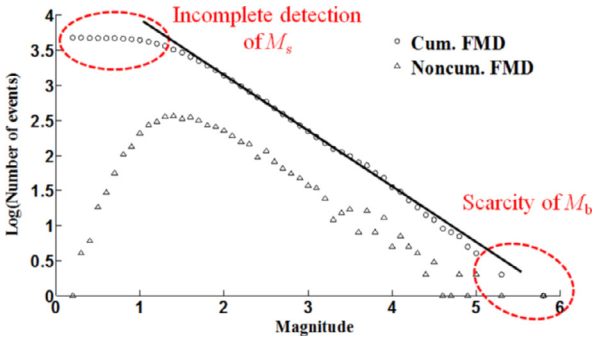

Fig. 1. The influence on the linearity of the magnitude–frequency distribution from scarcity of events with large magnitudes and incompleteness detection of events with small magnitudes.

the subduction rate [7], collapse analysis [8] and pore pressure variations. Since the higher levels of motion at a site are dominated by occurrences of the larger earthquakes, knowledge of the relation between *b*-value and large event is of great concern in seismic hazard analysis.

Due to the significance of the *b*-value, a reliable and accurate method to calculate the *b*-value appears very important. Actually, the linearity of Eq. (1) is not suitable well for all range of the magnitudes in the catalog. Deviation from linearity is believed to be due to statistical fluctuations of the scarcity of events with large magnitudes (denoted as M_b to large magnitude), or from the incompleteness of a detection threshold at small magnitude (denoted as M_s to small magnitude), as shown in Fig. 1.

Although events with M_b are scarce, they are the most important events to study, since they are the main sources of the seismic hazards. It is not reasonable for some author [9] to neglect these events in the calculation of the *b*-value. These events should be considered in the calculation and the deviation caused by M_b also needs to be reduced. To eliminate the deviation caused by M_s, the completeness magnitude M_c is usually to employ and events with magnitude smaller than M_c are not considered. Above M_c, all local events are detected, because they exceed the noise background on the seismogram. As magnitude decreases, however, events go undetected as the seismic signal approaches the noise background.

From the aforementioned description, how to determine M_c and how to reduce the effect of M_b play important roles in the calculation of *b*-value. Different from the traditional methods, least square regression (LSR) and maximum likelihood estimation (MLE) technique, a robust fitting method (RFM) to estimate the *b*-value was proposed in this paper. A reliable and stable *b*-value, with an ideal result to eliminate the effects from the M_b and M_c, can be estimated by RFM. Meanwhile, a new criterion to estimate M_c is offered. Finally, the variation of $b(t)$ as an earthquake precursor is discussed according to the introduced methods.

2. Description of the methods to estimate *b*-value of the Gutenberg (GR) law

The empirical validation of the universality hypothesis passes through the estimation of the *b*-value and its uncertainty. Different formulas were proposed in the past [10–15] which take into account the unavoidable binning of the magnitudes in different ways. Among these methods, least square regression (LSR) and maximum likelihood estimation (MLE) techniques are the most used.

2.1. Least square regression (LSR) technique

Typically, the *b*-value is extracted by performing least-squares linear regression on the logarithm of the histogram [12,16–22], although the use of the LSR does not have any statistical foundation.

LSR actually is a curve fitting technique. LSR minimizes the summed square of residuals *S*. The residual for the *i*th data point r_i is defined as the difference between the observed response value y_i and the fitted response value $\hat{y}_i$, and is identified as the error associated with the data. The summed square of residuals is given by

$$S = \sum_{i=1}^{n} r_i^2 = \sum_{i=1}^{n} (y_i - \hat{y}_i)^2, \tag{2}$$

where *n* is the number of data points included in the fit and *S* is the sum of squares error estimate. The least squares estimate of *b* is given by:

$$b_{\mathrm{LS}} = (\underset{\sim}{m}^T \underset{\sim}{m})^{-1} \underset{\sim}{m}^T \log \underset{\sim}{n}, \tag{3}$$

where the vector $\underset{\sim}{m} = (m_c, m_c + \Delta m, m_c + 2\Delta m, \ldots, m_{\max})$ contains the magnitudes of interest, and the vector $\log \underset{\sim}{n}$ gives the respective log number of earthquakes in the dataset greater than or equal to these magnitudes.

LSR works well under some circumstance, such as estimating the probability of the largest magnitude of earthquakes [15]. But it shows significant bias under relatively common conditions and some author [23] even suggested not using it.

2.2. Maximum likelihood estimation (MLE) technique

As an alternative, the maximum likelihood estimation method has been suggested to be preferable for calculating the *b*-value. In the first papers that described the MLE [10,13], the magnitude *M* was considered as a continuous random variable. If Eq. (1) holds, the probability density function (PDF) of *M* is

$$p(M) = b \ln(10) \frac{10^{-bM}}{10^{-bM_{\min}} - 10^{-bM_{\max}}}, \tag{4}$$

where $M_{\min}$ and $M_{\max}$ are, respectively, the minimum and the maximum magnitudes allowed. If $M_{\max} \gg M_{\min}$, Eq. (4) becomes

$$p(M) = b \ln(10) 10^{-b(M - M_{\min})}. \tag{5}$$

Note that the passage from Eq. (4) to Eq. (5) requires that, in practice, the Gutenberg (GR) law holds for a range of magnitudes $M_{\max} - M_{\min} \geq 3$ [10]. The MLE of Eq. (5) consists of choosing the *b*-value which maximizes the likelihood function [24], that is

$$b = \frac{1}{\ln(10)(\mu - M_{\mathrm{thresh}})}, \tag{6}$$

where μ is the sampling average of the magnitudes, and M_{thresh} is the threshold magnitude which usually corresponds to the minimum magnitude for the completeness of the seismic catalog. The error of the b-value is estimated by [14],

$$\sigma_b = 2.30b^2\sqrt{\frac{\sum_{i=1}^{N}(M_i-\mu)^2}{N(N-1)}}, \tag{7}$$

where N is the number of earthquakes.

The MLE is widely used and is accepted broadly among the existing methods. However, there are also problems for MLE and this will be discussed in part 3.

2.3. Robust fitting method (RFM)

LSR usually assumes that the response errors follow a normal distribution, and that extreme values are rare. Actually, extreme values called outliers do occur. According to the linearity of Eq. (1), M_b and M_c can both be taken as extreme values. To minimize the influence of outliers, the robust fitting method (RFM) is proposed, which has been used in other areas [25–28]. In RFM, robust bisquare weight least-squares regression is applied. This method minimizes a weighted sum of squares Eq. (2), where the weight given to each data point depends on how far the point is from the fitted line. Points near the line get full weight. Points farther from the line get reduced weight. Points that are farther from the line than would be expected by random chance get zero weight.

$$S_{\text{RFM}} = \sum_{i=1}^{n} w_i r_i^2 = \sum_{i=1}^{n} w_i (y_i - \hat{y}_i)^2, \tag{8}$$

where w_i are the weights. RFM with bisquare weights uses an iteratively reweighted least-squares algorithm, and follows this procedure:

(1) Fit the model by weighted least squares.

(2) Compute the adjusted residuals and standardize them. The adjusted residuals are given by

$$r_{\text{adj}} = \frac{r_i}{\sqrt{1-h_i}}, \tag{9}$$

where r_i are the usual least-squares residuals and h_i are leverages that adjust the residuals by downweighting high-leverage data points, which have a large effect on the least-squares fit. The standardized adjusted residuals are given by

$$u = \frac{r_{\text{adj}}}{K \cdot \text{MAD}}, \tag{10}$$

where K is a constant equal to 6.946, and MAD is the median absolute deviation of the residuals.

(3) Compute the robust weights as a function of u. The bisquare weights are given by

$$w_i = \begin{cases} (1-(u_i)^2)^2 & |u_i| < 1 \\ 0 & |u_i| \geq 1 \end{cases}. \tag{11}$$

(4) If the fit converges, then you are done. Otherwise, perform the next iteration of the fitting procedure by returning to the first step.

3. The comparisons of the three models in the calculations of *b*-value

For comparison of the three methods to estimate b-value, central regional (from latitude 20°N to 45°N and longitude 80°E to 100°E) catalog of China for the period between 29th October 2010 and May 13th 2011with 4736 events was analyzed. The analysis is focused on the aforementioned effects of M_c and M_b.

3.1. The effect of the minimum magnitude of complete recording M_c

The minimum magnitude of complete recording M_c is an important parameter for most studies related to seismicity, especially for the estimation of the b-value. Variations of b-value with different assumed M_c are investigated for the three methods. The value of the assumed M_c starts from the minimum magnitude in the catalog and increases gradually, and the corresponding $b(M_c)$ is calculated simultaneously. The effects of the minimum magnitude of complete recording M_c for the three methods are shown in Figs. 2–4.

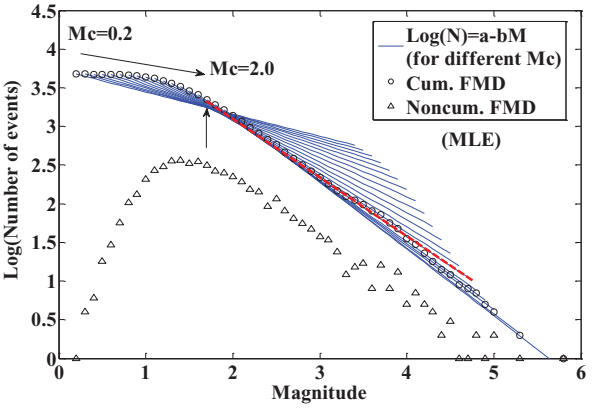

Fig. 2. The influence of M_c (from 0.2 to 2.0) on the estimation of b-value for MLE. Choice of best model from the MLE denotes by the red dashed line and the M_c by the arrow upward. (For interpretation of the references to color in this figure legend, the reader is referred to the web version of this article.)

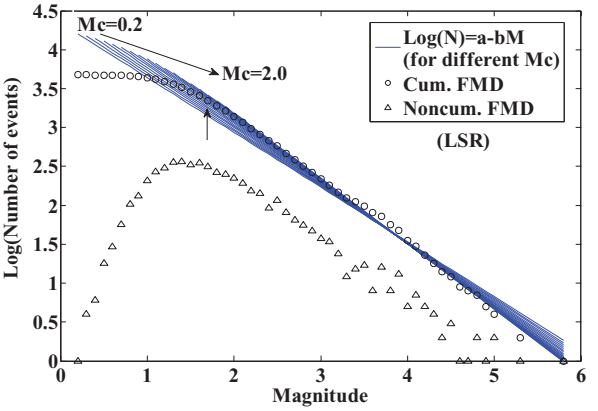

Fig. 3. The influence of M_c (from 0.2 to 2.0) on the estimation of b-value for LSR. The upward arrow points out the best M_c for the catalog.

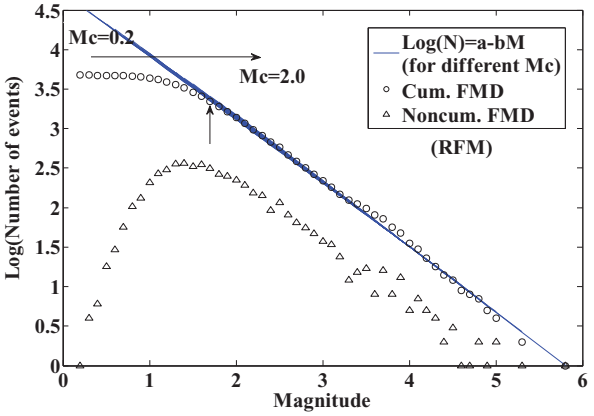

Fig. 4. The influence of M_c (from 0.2 to 2.0) on the estimation of b-value for RFM. The upward arrow points out the best M_c for the catalog.

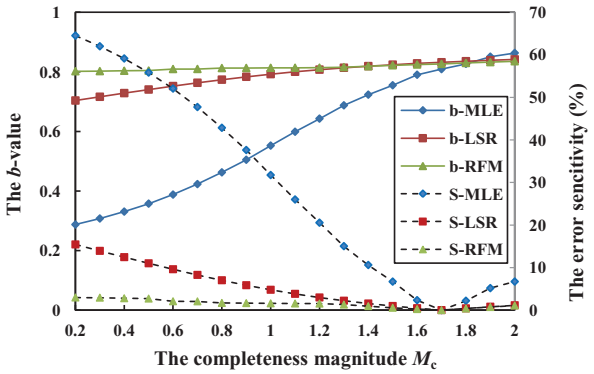

Fig. 5. The b-value and error sensitivity $S^b_{M_c}$ of LSR, MLE and RFM methods. Note the real completeness magnitude $M_{c\text{-best}}$ is equal to 1.7 and its corresponding b-value is b_{best}.

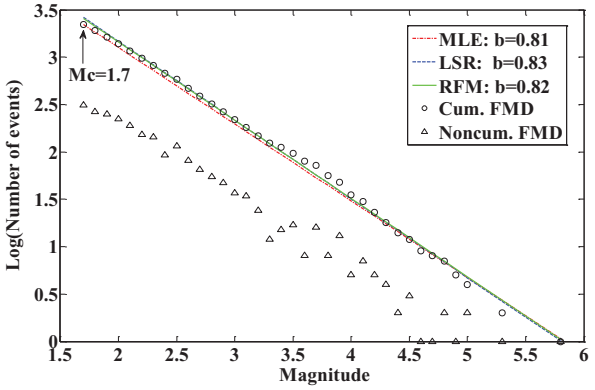

Fig. 6. The influence of M_b on the estimation of b-value for LSR, MLE and RFM. In this condition all data with magnitude $\geq M_{c\text{-best}}$ are considered.

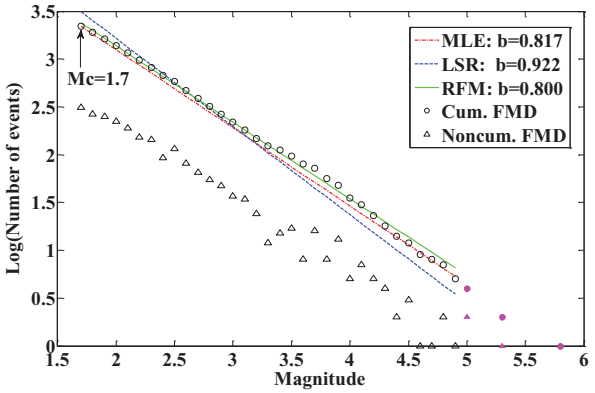

Fig. 7. The influence of M_b on the estimation of b-value for LSR, MLE and RFM. In this condition all data with magnitude $\geq$5.0 (the filled points) are not considered.

As shown in Figs. 2–4, different methods show different sensitivities to the change of M_c. In order to operate quantitative analysis, the absolute-sensitivity of b-values to the variations of M_c is defined as follows:

$$S^b_{M_c} = \frac{|b_{M_c} - b_{best}|}{b_{best}} \times 100\%, \tag{12}$$

where $S^b_{M_c}$ reflects the error sensitivity of M_c for the calculation of b-value, and b_{best} is the value corresponding to the actual or best completeness M_c (denoted by $M_{c\text{-best}}$) of the catalog. Obviously, the smaller the value of $S^b_{M_c}$ is, the more accurate b-value we will get, and the corresponding M_c is more close to $M_{c\text{-best}}$. The results of $S^b_{M_c}$ for the three models are shown in Fig. 5.

As shown in Fig. 5, the MLE is excessively sensitive to the change of M_c. A minute change $\Delta M_c = 0.1$ from $M_{c\text{-best}}$ leads to almost 5% of the change of error sensitivity. When ΔM_c becomes bigger, the error in the estimation increases sharply. The result from LSR is better than that in MLE. As for RFM, the estimate offers a robust and stable result when M_c changes. The influence from a big change $\Delta M_c = 0.6$ or bigger can be neglected compared with the results from the LSR and MLE. This robust characteristic of RFM is very useful, especially when $M_{c\text{-best}}$ is not obtained accurately. Actually, there is no method that can guarantee to give exact $M_{c\text{-best}}$ due to different complicated conditions and usually an approximate value is employed.

3.2. *The effect of the scarcity of events with* M_b

The other deviation from linearity is the scarcity of events with large magnitude (M_b). A simple way to eliminate the effect from M_b is to not consider these events in calculation, just as the research in [9]. However, M_b event plays a dominated role in the destruction estimation and the relation between the variation of b-value and M_b event seems to be very important. The method by simply eliminating M_b is obviously not to be acceptable. In order to better investigate $b(M_b)$, we consider the events with magnitude $\geq M_{c\text{-best}}$ and the M_b events are eliminated from the catalog gradually from 5.8 to 4.3 to simulate the occurrence of different large events and the corresponding b-value is calculated. The results are shown in Figs. 6–8.

As shown in Figs. 6–8, during the change of M_b events, the MLE and RFM can keep the linear property well, whereas the LSR seems to have a great deviation. Similarly, $S^b_{M_b}$ is employed here in Eq. (13) with the similar definition in Eq. (12) to reflect the effect of the b-value for the occurrence of M_b for

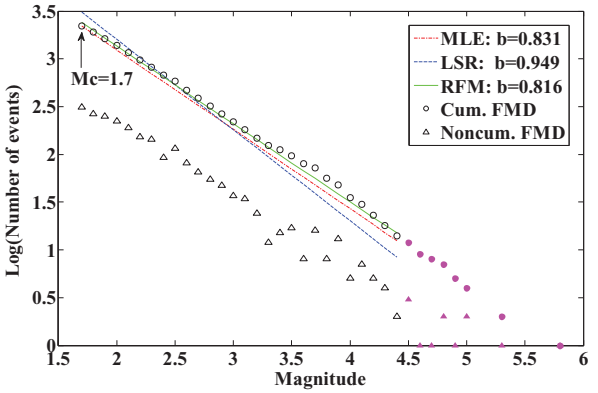

Fig. 8. The influence of M_b on the estimation of b-value for LSR, MLE and RFM. In this condition all data with magnitude ≥4.5 (the filled points) are not considered.

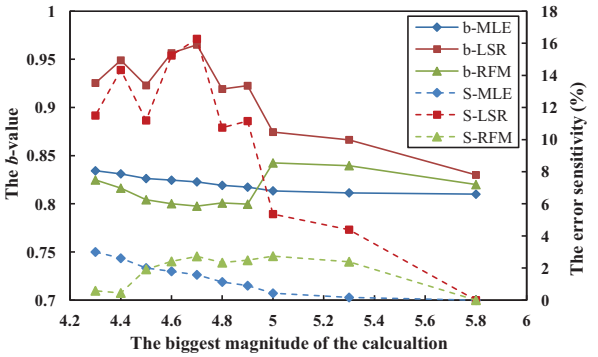

Fig. 9. The b-value and error sensitivity $S^b_{M_b}$ of LSR, MLE and RFM models. Note the value of x-axis corresponding to the biggest magnitude of the events for calculation. The b_{best} here is the value for $x = 5.8$.

the three methods.

$$S^b_{M_b} = \frac{|b_{M_b} - b_{best}|}{b_{best}} \times 100\% \tag{13}$$

As shown in Fig. 9, MLE almost has no sensitive to the occurrence of large events with $M \geq 5.0$. Since whether the biggest events with $M = 5.8$ happen or not, the b-value changes very minute, even events with magnitude ≥5.0 occurrence just cause 0.17% variation. The variation of b-value in MLE is less sensitive to the large events. For the LSR, the $S^b_{M_b}$ value changes abruptly and shows an unstable and random trend. Such as whether the biggest events M=5.8 happen or not can cause more than 4% variation. This change can happen not only for the bigger event, but for any outlier event. Thus the big variation of LSR is not always related to the occurrence of the large events, which may provide wrong information to us. As for RFM, it not only can reflect the impact of the large events properly, but also can keep the linear property well.

3.3. The "weighted" analysis of the three methods

From the aforementioned description, the main disadvantage of LSR is its sensitivity to large events (outliers). Outliers have a large influence on the fit because squaring the residuals in Eq. (2) magnifies the effects of these extreme data points. In this aspect, LSR gives too heavy weight to the points of outliers and causes great deviation from the linearity of Eq. (2). The real meaning of the b-value from LSR for Eq. (2) might be questionable. This is supported by the study of [29]. The biases in the estimation of the b-value of the Gutenberg (GR) law and of its uncertainty though LSR were investigated conceptually, analytically and numerically and suggested that the LSR will never be used in the future. According to the above characteristic of LSR, we also suggest not to use it if there is a better method.

MLE is the most used method to estimate the b-value in the present research. It is necessary to give a detailed analysis. MLE is based on the assumption that the magnitude M was considered as a continuous random variable. But this approximation can be strictly justified only for $\Delta M \to 0$. As a matter of fact, the magnitude is not a continuous variable and it is unavoidable to have measurement errors. In practical cases, the uncertainties on the measured magnitudes lead to the use of "binned" magnitudes, i.e. the magnitudes are grouped by using a selected interval ΔM. For instance, for instrumental measurements, the magnitude interval used for the grouping is $\Delta M = 0.1$, and for magnitude estimation of historical events, the grouping can even be $\Delta M \geq 0.5$.

From Eq. (6), the b-value from MLE depends on two factors: the average μ and M_{thresh} (M_{thresh} is the same as $M_{c\text{-}best}$). The sample average μ computed from binned data is systematically higher than the true value μ. This is due to the fact that the real (continuous) magnitudes in the interval $M_i - \Delta M/2 \leq M < M_i + \Delta M/2$ are not symmetrically distributed around the central value M_i. So this produces a biased estimation of the real b-value. The bias is negligible for $\Delta M = 0.1$, while it is very important for larger ΔM (for example, $\Delta M = 0.6$), that might be necessary to evaluate the b-value for historical catalogs [12].

For M_{thresh}, usually $M_{thresh} \neq M_{min}$ will also cause bias for the estimation of b-value. Since the lowest binned magnitude, i.e. the threshold magnitude, contains all the magnitudes in the range $M_{thresh} - \Delta M/2 \leq M < M_{thresh} + \Delta M/2$, then $M_{min} = M_{thresh} - \Delta M/2 < M_{thresh}$ (*e.g.*, [12]). So a slight modification of Eq. (6) is suggested [15],

$$b = \frac{1}{\ln(10)\left[\mu - (M_{thresh} - \Delta M/2)\right]}. \tag{14}$$

Remarkably, this "corrected" formula was not largely employed. Whereas the difference between (6) and (13) is certainly considerable because in a power law distribution the average μ is very close to the minimum value of the distribution.

$$\mu = b\ln(10)\int_{M_{min}}^{\infty} M10^{-b(M-M_{min})} \cdot dM = M_{min} + \frac{1}{b\ln(10)}. \tag{15}$$

In particular,

$$\Delta b = \text{Eq. (13)} - \text{Eq. (6)} = \frac{\Delta M/2}{\ln(10)[(\mu - M_{thresh})(\mu - M_{thresh} + \Delta M/2)]}. \tag{16}$$

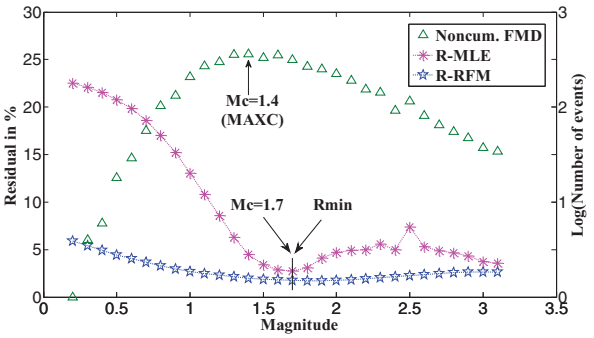

Fig. 10. The application of the proposed method to estimate M_c in MLE and RFM. The MAXC is maximum curvature method which takes the magnitude with maximum number as M_c.

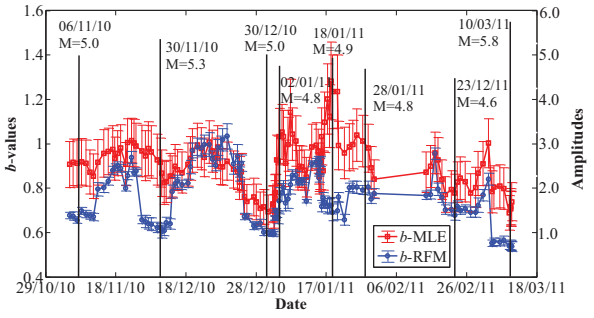

Fig. 11. The b-values (left scale) as a function of window number or time. Solid, vertical lines represent time of occurrence and magnitude (right scale) of all recorded earthquakes with $M_w > 4.5$. Vertical bars indicate one standard deviation of the b-value.

For $\Delta M = 0.1$ (as for instrumental magnitudes), and $\mu - M_{\text{thresh}} \approx 0.38$ (obtained by Eq. (15) with $b = 1$) we obtain $\Delta b \approx 0.13$.

Besides, for Eq. (6) or Eq. (14), the b-value is determined only by sample average μ when M_{thresh} is known. Parameter μ is related with the amplitudes and their corresponding numbers. The number of each amplitude actually plays the role of the weight function. For the earthquakes, the small events happen more frequently than the large events, so the number of small events located near M_c is far greater than the number of the large events. μ is mainly affected by the small events, which can be reflected in Eq. (15). This can explain why a little change of magnitude in the small value can cause great variation in the b-value, see Fig. 2 and why it almost has no sensitivity to the change of M_b, see Fig. 10. MLE weights too much for the small events. From the practical point of view, the too much weight for the small events makes the b-value too sensitive to the determination of M_c. Meanwhile the less weight for the large event makes the function of b-value as an earthquake precursor is greatly reduced, which will be seen in Fig. 11.

4. The methods to estimate M_c of the catalog

From the aforementioned analysis, a reliable M_c determination is necessary for the calculation of the b-value, especially for MLE. The assessment of the magnitude of completeness, M_c, which is defined as the lowest magnitude at which 100% of the events in a space–time volume are detected [30–32]. The definition is not strict in a mathematical sense, and is connected to the assumption of a power-law behavior of the larger magnitudes. If we choose a too low value for M_c we will get a biased estimate of the scaling parameter since we will be attempting to fit a power-law model to non-power-law data. On the other hand, if we choose a too high value for M_c we are effectively throwing away legitimate data points $M_i < M_{\text{min}}$, which increases both the statistical error on the scaling parameter and the bias from finite size effects. The goal is to find a good compromise between these cases.

It is further complicated by the need to determine M_c automatically, since in most applications, numerous determinations of M_c are needed when mapping parameters such as seismicity rates or b-values.

Some methods are already proposed, such as Entire-magnitude-range method (EMR) [33], maximum curvature method (MAXC) [31], goodness-of-fit test [31], day–night difference sensitivity [30], the seismic-station sensitivity method [34] and so on. In this study, a new method to estimate the M_c is proposed.

Our estimate of M_c is based on the assumption of the magnitude-frequency distribution (FMD) of Eq. (1). To evaluate the accuracy of M_c, we compute the difference between the observed FMD and a synthetic distribution. For incomplete data sets, a simple power-law cannot adequately explain the observed FMD, so the difference will be high. The following steps are taken to estimate M_c: first we estimate the b- and a-values of the Gutenberg (GR) law as a function of minimum magnitude, based on the events with $M \geq M_i$. We use RFM (or MLE) to estimate the b- and a-values. Next, we compute a synthetic distribution of magnitudes with the same b-, a- and M_i values, which represents a perfect fit to a power law. To estimate the accuracy of M_c we compute the absolute residual, R, of the logarithm number of events in each magnitude bin between the observed and synthetic distribution

$$R(a, b, M_i) = \frac{\sum_{M_i}^{M_{\max}} |\log_{10} O_i - \log_{10} S_i|}{\sum_i \log_{10} O_i} \times 100\%, \qquad (17)$$

where O_i and S_i are the observed and predicted cumulative number of events in each magnitude bin, respectively. We divide by the total logarithm number of observed events to normalize the distribution.

Our method is illustrated in Fig. 10, which shows R as function of M_i. If M_i is smaller than $M_{\text{c-best}}$, the synthetic distribution based on a simple power-law cannot model the FMD adequately and, consequently, the difference between the observed FMD and synthetic distribution is high. The absolute residual value R, measuring the accuracy of M_c, decreases with increasing M_i and reaches a minimum value at $M_{\text{c-best}}$. Just as shown in Fig. 10, when $M_i = M_{\text{c-best}}$ (=1.7), the residual reaches the minimum value both in RFM and MLE. Beyond $M_{\text{c-best}}$, R increases gradually. Therefore, the M_i value corresponding to the minimum value of R can be taken as the magnitude of completeness $M_{\text{c-best}}$.

5. *b*-Value as an earthquake precursor

A *precursor phenomenon* is one which occurs before a mainshock and is a part of a physical preparation for the main rupture; it does not simply mean "before" but it implies casual linkage to the mainshock [35].

Seismic precursory phenomena e.g. changes of seismic quiescence (periods when seismicity rate decreases to levels significantly below the normal seismicity rate), changes in the source parameters of events and changes in the frequency magnitude distribution (FMD) have been proposed by many investigators as precursors [36–42].They suggest that detection of seismic quiescence based on uninterrupted observation is a key to the success of earthquake prediction.

Most of the methods described as successfully predicting earthquakes have been applied after the fact. It is actually quite difficult to assess if a general method is statistically successful or not. The incentive of this part is to examine retrospectively the potential of temporal *b*-variations as an earthquake precursor for large earthquakes.

The study focuses on the determination of the *b*-value as a function of time and on the assessment of its potential as an earthquake precursor. To study variations of *b*-value with time, a sliding time-window method is used. A group of earthquakes is chosen from an earthquake catalog. The *b*-value is calculated for the first N events. Then, the window is shifted by a time corresponding to certain number of events, e.g. $N/10$ events. The *b*-value is calculated for the new group of data and the process is repeated until the last event is reached. Every calculated *b*-value is assigned to the middle time of the corresponding window.

The $b(t)$ in our study is calculated based on the earthquake data of the previous central region catalog using a sliding time-window containing 100 events and a 10 events shift. The chosen number of events in the window is a compromise between the time resolution and smoothing effect of broad windows. The temporal variation, $b(t)$, is studied using the MLE and RFM techniques, described in Section 2 simultaneously and the results are shown in Fig. 11.

On the whole, the two methods studied show similar results. Statistically significant drops in *b*-value reveal an V-shape curve in the $b(t)$ diagrams. The *b*-value decreases significantly prior to the occurrence of large earthquakes. Results show that large earthquakes are often preceded by a medium-term increase in *b*, followed by a decrease in short-time before the earthquake, which is in accordance with the result in [43]. Most of the associated seismicity takes place close to the minima in the $b(t)$-curve.

During the reviewed time period, there are at least six drops of $b(t)$ in Fig. 11. It can be seen that in most cases there is a good agreement between a sudden significant decrease in the $b(t)$ curve and the subsequent occurrence of large earthquakes ($M > 4.5$). The variation of *b*-value in Fig. 11 reveals stronger correlation between a sudden decrease in $b(t)$ and a successive increase of seismicity. This phenomenon is clear in the diagrams for each method. From this point of view, the variations of *b*-value in time as earthquake precursors are successful for both methods.

However, if we give a detailed study for the two methods, the difference is obvious. Firstly, the standard deviations shown as the error bars in Fig. 11 of the two methods are different. The standard deviation value of the MLE is almost four times bigger than that in RFM. This means the *b*-value calculated from RFM is more stable and reliable than that from MLE.

Secondly, although the global change trends of $b(t)$ are similar, the change amplitudes are different. The *b*-value varies from 0.7 to 1.3 for the MLE, while RFM has the trend with *b*-value ranging about 0.5–1. In Fig. 11, we can see that the RFM is more sensitive to the occurrence of large earthquakes. Two large events, one happened on 30/11/2010 with $M = 5.3$ and the other happened on 30/12/2010 with $M = 5.0$, are chosen for a detailed study. For RFM the *b*-values of foreshocks drop by about 50%, whereas the bigger drop for the RFM is less than 30%. This can be understood by the analysis in Section 2 , since MLE is less sensitive to the large events than the other two methods.

Thirdly, seven out of eight events in RFM with $M > 4.5$ occurred within the low or minimum *b*-values time, except the event happened in 02/01/2011 with M=4.8. However, in these eight events, only four events in 30/11/2010, 30/12/2010, 23/12/2011 and 10/03/11 happened in its low values for MLE. For the event happened in 02/01/11, the corresponding *b*-value of both methods lies in the increasing part. This can be explained by combining the three days earlier event in 30/12/10, the event in 02/10/11 played the role of the aftershock or emerged in the aftershocks.

From the above three aspects, it is obviously that from the earthquake precursor point of view, the variations of $b(t)$ calculated from the RFM is more efficient than that from the MLE. The merit of RFM is conformed one time again.

6. Conclusion

Since the magnitude-frequency distribution was proposed by Gutenberg and Richter [2] in 1944, the Gutenberg (GR) law has been widely used in the earthquakes research. The parameter *b* in the law attracts more researchers' interest and is demonstrated to be a useful parameter in many applications. Two mainly used methods, LSR and MLE to calculate the *b*-value are analyzed in this study. LSR is affected greatly by the outliers, and cannot always give the reliable result. The fitting line always has a great deviation from the real linearity relation and it is suggested not to be used in the future. As for MLE, it is widely accepted in the present study. However, MLE gives too much weight for the small events and its sensitivity to the completeness amplitude M_c is very extensive. Thus *b*-value from MLE may have a great deviation from the real value when M_c is not determined accurately. On the other hand, the sensitivity of MLE to the occurrence of events with large magnitude is minute, since large events gain far smaller weight in the *b*-value calculation. Therefore, the function of $b(t)$ from MLE as an earthquake precursor is greatly influenced. According to the problems existed in the abovementioned methods, the robust fitting method (RFM) was proposed to calculate *b*-value in this paper. RFM gives different weights to the points according to their distances from the linear fitted line. Points near the line get full weight, whereas points far from the line get reduced weight. As a result, RFM can not only provide a stable and reliable *b*-value without the strict requirement for $M_{c\text{-best}}$ like MLE, but also

has a good sensitivity to the occurrence of earthquakes with large magnitudes.

The concept of variations of b-value in time as earthquake precursors was successfully applied for tectonic earthquakes in the central region of China. Results show that calculated b-value shows large time variations. Almost all statistically significant drops in b-value can be associated with an occurrence of large shocks ($M > 4.5$) in our study. A rapid increase of $b(t)$ is observed after the occurrence of large earthquakes. This typical phenomenon is observed in $b(t)$ plots for most of the large earthquakes. Variations of b-value in time can be used as earthquake precursors. Compared with the traditional method MLE, the variation of b-value from RFM is shown to be more effective as an earthquake precursor.

Acknowledgments

The authors of this paper would like to express their appreciation for the financial support given by the National Natural Science Foundation of China (No. 51408408).

References

[1] Rydelek PA, Sacks IS. Comment on "Minimum magnitude of completeness in earthquake catalogs: examples from Alaska, the Western United States, and Japan". Bull Seismol Soc Am 2003;93:1862–7.
[2] Gutenberg B, Richter CF. Frequency of earthquakes in California. Bull Seismol Soc Am 1944;34:185–8.
[3] Allen CR, Amand PS, Richter CF, Nordquist JM. Relationship between seismicity and geologic structure in the Southern California Region. Bull Seismol Soc Am 1965;55:753–97.
[4] Smith WD. The b-value as an earthquake precursor. Nature 1981;289:136–9.
[5] Mogi K. Study of elastic shocks caused by the fracture of heterogeneous materials and its relations to earthquake phenomena. Bull Earthq Res Inst 1962;40:125–73.
[6] Scholtz CH. The frequency–magnitude relation of microfracturing in rock and its relation to earthquakes. Bull Seismol Soc Am 1968;58:399–415.
[7] Cao AM, Gao SS. Temporal variations of seismic b-values beneath Northeastern Japan island arc. Geophys Res Lett 2002;29.
[8] Carpinteri A, Lacidogna G, Puzzi S. From criticality to final collapse: evolution of the b-value from 1.5 to 1.0. Chaos Solitons Fractals 2009;41:843–53.
[9] Khan PK, Chakraborty PP. The seismic b-value and its correlation with Bouguer gravity anomaly over the Shillong Plateau area: tectonic implications. J Asian Earth Sci 2007;29:136–47.
[10] Aki K. Maximum likelihood estimate of b in the formula $\log(N) = a - bM$ and its confidence limits. Bull Earthq Res Inst Tokyo Univ 1965;43:237–9.
[11] Tinti S, Mulargia F. Confidence intervals of b-values for grouped magnitudes. Bull Seismol Soc Am 1987;77:2125–34.
[12] Bender B. Maximum likelihood estimation of b values for magnitude grouped data. Bull Seismol Soc Am 1983;73:831–51.
[13] Utsu T. A method for determining the value of b in a formula $\log n = a - bM$ showing the magnitude–frequency relation for earthquakes. Geophys Bull 1965;13:99–103.
[14] Shi Y, Bolt BA. The standard error of the magnitude–frequency b-value. Bull Seismol Soc Am 1982;72:1677–87.
[15] Utsu T. A statistical signficance test of the difference in b-value between two earthquake groups. J Phys Earth 1966;14:34–40.
[16] Page R. Aftershocks and microaftershocks of the Great Alaska earthquake of 1964. Bull Seismol Soc Am 1968;58:1131–68.
[17] Main I. Apparent breaks in scaling in the earthquake cumulative frequency–magnitude distribution fact or artifact? Bull Seismol Soc Am 2000;90:86–97.
[18] Triep EG, Sykes LR. Frequency of occurrence of moderate to great earthquakes in intracontinetal regions: implications for changes in stress, earthquake prediction, and hazard assessment. J Geophys Res 1997;102:9923–48.
[19] Okal EA, Kirby SH. Frequency–moment distribution of deep earthquake; implications for the seismogenic zone at the bottom of Slabs. Phys Earth Planet Inter 1995;92:169–87.
[20] Karnik V, Klima K. Magnitude–frequency distribution in the European–Mediterranean earthquake regions. Tectonophysics 1993;220:309–23.
[21] Pacheco JF, Sykes LR. Seismic moment catalog of large shallow earthquakes, 1900 to 1989. Bull Seismol Soc Am 1992;82:1306–49.
[22] Scholtz CH. Size distributions for large and small earthquakes. Bull Seismol Soc Am 1997;87:1074–7.
[23] Marzocchi W, Sandri L. A review and new insights on the estimation of the b-value and its uncertainty. Ann Geophys 2003;46:1271–82.
[24] Fisher RA. Contribution to mathematical statistics. New York: Wiley; 1950.
[25] Rousseeuw P.J., Leroy A. Robust regression and outlier detection. John Wiley & Sons, New York.1987.
[26] Nesi P, Bimbo AD, Ben-Tzvi D. A robust algorithm for optical flow estimation. Comput Vis Image Underst 1995;62(1):59–68.
[27] Danuser G, Stricker M. Parametric model fitting: from inlier characterization to outlier detection. IEEE Trans. Pattern Anal Mach Intell. 1998;20(2):263–80.
[28] Wang H, Suter D. MDPE: a very robust estimator for model fitting and range image segmentation". Int J Comput Vis 2003;59(2):139–66.
[29] Sandri L, Marzocchi W. A technical note on the bias in the estimation of the b-value and its uncertainty through the least squares technique. Ann Geophys 2007;50:329–39.
[30] Rydelek PA, Sacks IS. Test the completeness of earthquakes catalogue and the hypothesis of self-similarity. Nature 1989;337:251–3.
[31] Wiemer S, Wyss M. Minimum magnitude of complete reporting in earthquake catalogs: examples from Alaska, the Western United States, and Japan. Bull Seismol Soc Am 2000;90:859–69.
[32] Taylor SR, Snoke JA, Sacks IS, Takanami T. Nonlinear frequency–magnitude relationship for the Hokkaido corner, Japan. Bull Seismol Soc Am 1990;80:340–53.
[33] Ogata Y, Katsura K. Analysis of temporal and spatial heterogeneity of magnitude frequency distribution inferred from earthquake catalogs. Geophys J Int 1993;113:727–38.
[34] Dent VF. Seismic network capability and magnitude completeness maps, 1960–2005 for Western Australia, South Australia and the Northern Territory. In: Proceedings of American Ecology Engineering Society conference. Melbourne; 2009.
[35] Wyss M, Habermann RE. Seismic quiescence precursory to a past and a future Kurile island earthquake. Pure Appl Geophys 1979;117:1195–211.
[36] Enescu B, Ito K. Spatial analysis of the frequency–magnitude distribution and decay rate of the 2000 Western Tottori earthquake. Earth Planets Space 2001;54:847–60.
[37] Wiemer S, Yoshida A, Hosono K, Nogichi S, Takayama H. Correlating seismicity parameters and subsidence in the Tokai region, Central Japan. J Geophys Res 2005;110.
[38] Schorlemmer D, Wiemer S, Wyss M. Earthquake statistics at Parkfield I: stationarity of b-values. J Geophys Res 2003;109.
[39] Huang Q, Oncel AO, Sobolev GA. Precursory seismicity changes associated with the Mw = 7.4 1999 August 17 Izmit (Turkey) earthquake. Geophys J Int 2002;151:235–42.
[40] Monterroso DA, Kulhánek O. Spatial variations of b-values in the subduction zone of Central America. Geofis Int 2003;42:1–13.
[41] Nuannin P, Kulhánek O, Persson L. Spatial and temporal b-value anomalies preceding the devastating off coast of NW Sumatra earthquake of December 26, 2004. Geophys Res Lett 2005;32:L11307.
[42] Jia L, Lin H, Duan Z. Convex set theory-based seismic hazard analysis of low seismicity area. Soil Dyn Earthq Eng 2011;31:463–9.
[43] Sammonds PR, Meredith PG, Main IG. Role of pore fluid in the generation of seismic precursors to shear fracture. Nature 1992;359:228–30.